epl draft

Thermodynamic theory of voting and EU elections

Klaus M. Frahm[1] and Dima L.Shepelyansky[1]

[1] *Univ Toulouse, CNRS, Laboratoire de Physique Théorique, Toulouse, France*

*** Missing PACS ***

Abstract –We introduce a thermodynamic theory of voting and show that it provides a good description of distribution of party votes in EU elections. The theory traces parallels between system energies of coupled nonlinear oscillators and party vote fractions. Such a classical system evolution is characterized by the conservation of total energy and probability norm that leads to the Rayleigh-Jeans (RJ) thermalization and condensation at low energy states. A similar thermalization also describes the wealth inequality in society. This feature belongs to the phenomena of constraint driven condensation known in statistical mechanics. We show that the RJ theory well depicts the Lorenz and Pareto curves obtained from the EU vote results. The theory also recovers the dispersion of votes between candidates of first round presidential elections in France.

Introduction. – In the European Union (EU) elections to the European Parliament take place every five years by universal adult suffrage with more than 400 million people eligible to vote [1,2]. The campaigns of political parties still take place through national elections even if political parties have the right to campaign EU-wide. The country election system is a form of proportional representation of parties. The electoral threshold, if any, may not exceed 5%. There is only one election round at which a rather high number of parties, typically between 20 and 40, participate.

In this work, we use the EU public election results [1,2] and present their statistical distribution of party votes for the time period from 1994 to 2024 (for France and Germany) and for top 10 EU countries by population for 2024 (DE, FR, IT, ES, PL, RO, NL, BE, SE, CZ; here countries are given by their alpha-2 codes ISO 3166-1). We also consider the French 1st round presidential elections since 1965 [3]. To characterize the properties of this distribution, we use a description based on the Lorenz curve which gives the dependence of cumulated normalized wealth (vote fractions here) $0 \leq w \leq 1$ on the cumulated normalized fraction of population or households (political parties or electoral candidates here) $0 \leq h \leq 1$ [4]. The case of perfect equipartition (identical vote fractions for all parties) corresponds to the diagonal $w = h$ and the doubled area between diagonal and the Lorenz curve $w(h)$ gives the Gini coefficient $0 \leq G \leq 1$ [5,8] which is broadly used in the studies of wealth inequality in world countries [6–8].

The striking feature of wealth inequality is that for the whole world 50% of the population owns only 2% of total wealth, while 10% (1%) of the riches population owns 75% (38%) of the total wealth [7]. In [9,10] it was shown that this inequality can be naturally explained by the Rayleigh-Jeans (RJ) thermalization (see e.g. [11,12]) that leads to RJ condensation (RJC) and the formation of a huge poverty phase of low wealth and a tiny oligarchic phase that captures the main part of total society wealth. It is also argued that the RJC phenomenon describes the energy and carbon emission distribution between the world countries [13].

In physical systems RJC is also observed in multimode optical fibers [14–18]. This is a specific case of a more generic phenomenon known in statistical mechanics as constraint-driven condensation [19–21] that is universal and exists for such systems as coalescence in granular media, jamming in traffic, gelation in networks [20] and financial data analysis [21]. RJC also exists in systems of dynamical chaos where moderate nonlinear couplings between oscillators lead to RJ thermalization [9,10,18,22].

In previous works RJ thermalization and condensation were considered for some physical objects like light intensity in fibers, wealth, energy or carbon emission [9,10,13]. Here we develop the Thermodynamic Theory of Voting (TTV) according to which opinion formation and Vote Preferences (VP) result from certain complex interactions between agents/electors in a society that leads to a thermal distribution of votes between parties participating in elections. Of course, it is assumed that the number of parties is significantly higher than two. We show that the TTV approach gives a good description for the party/competitors distribution of votes in EU elections and also in the first round presidential elections in France.

We point out that there is a developed mathematical theory of voting with many nontrivial results (see e.g. [23–26]). But there the electors are usually considered as independent noninteracting agents. In contrast to this, in the TTV approach it is assumed that there are certain couplings and nonlinear interactions between electors operating in the framework of classical mechanics. This leads to thermalization of voting with the emergence of RJ distribution of votes between parties. In a certain sense this process is similar to the thermalization of interacting atoms in a three-dimensional box: almost any interactions lead to a thermal steady-state with average energy $3T/2$ given by temperature T [11] with the Boltzmann constant taken here as unity (but no themalization happens without nonlinear interactions). We show that the TTV concept provides a detailed statistical description of real results of EU and other elections.

We also note that there are various physical models of opinion formation and voting of interacting agents (see e.g. [27–30] and Refs. therein) but they do not yet describe the results of real elections.

RJC and Lorenz, Pareto curves construction. – Yakovenko et al. [31, 32] proposed to use the statistical Boltzmann-Gibbs (BG) approach to describe the distribution of money, wealth and income in terms of an exponential function depending on the temperature parameter T. However, it happens that in this case the Lorenz curve does not depend on T and has always the same Gini coefficient $G = 0.5$ [10, 32]. Therefore, in [32], an extension was proposed where the tail of the BG distribution is replaced by a power law tail, according to the Pareto distribution. This procedure appears to be somewhat artificial and does not seem to be natural.

A different view point is given by the Wealth Thermalization Hypothesis (WTH), introduced in [9, 10], which is based on the idea of the conservation of two quantities as it was argued in [33, 34] in the context of wealth distribution. This approach assumes that the wealth in a country is analogous to the global energy of a certain (chaotic) classical oscillator system with specific weak nonlinear interactions between the oscillators such that there are indeed two integrals of motion which are the global energy E and the global norm, given as the sum of all squared oscillator amplitudes. Such a system thermalizes under certain conditions [9] and in this case for each oscillator at energy (frequency) E_m, the statistical average of its norm probabilities (squared amplitudes) is given by the RJ expression [11, 12]:

$$\rho_m = \frac{T}{E_m - \mu} \text{ (RJ)} . \quad (1)$$

Historically, this expression describes the thermalization of classical fields. In the context of the WTH, ρ_m represent averaged stationary probabilities at certain wealth states $0 \leq m < N$ with wealth/energies $w_m = E_m$. The two parameters T and μ are the system temperature T and the chemical potential $\mu(T)$ which are determined by the two implicit equations $E = \sum_m E_m \rho_m$ and $\eta = \sum_m \rho_m = 1$ (at a given value of the global energy E and for a given oscillator spectrum E_m; see [9] for details).

In this work, we extend the ideas of the WTH to elections (TTV approach) where the vote fractions V_m correspond to wealth or energy $w_m = E_m = V_m$ (in the following, we usually use equivalently these three quantities) and political parties or election candidates corresponding to (vote fractions) of population (or occupation probabilities for certain oscillator modes).

The important feature of the RJ distribution (1) is the possible condensation of a macroscopic part of the total probability η at the lowest energy state with E_0 (or few lowest states E_m) provided the global energy or temperature is sufficiently low, $E \sim E_1 - E_0$ or $\varepsilon \ll 1$. Here $\varepsilon = E/B$ is the rescaled energy and $B = E_{N-1}$ is the energy bandwidth (in this work, we assume $0 = E_0 < E_1 < \ldots < E_{N-1} = B$ and we usually choose models with $B \approx 1$).

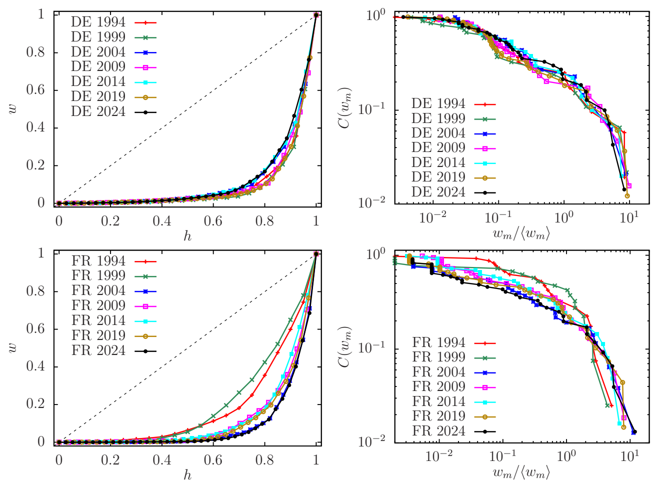

Fig. 1: (Color on-line) *Left:* Lorenz curves of EU elections of Germany (DE; top) and France (FR, bottom) since 1994. The x-axis corresponds to the cumulated fraction of households/political parties (h) and the y-axis to the cumulated fraction of wealth/obtained votes (w). The dashed black line corresponds to the line of perfect equipartition $w = h$. The Gini coefficients G and number of political parties N_p for all cases can be found in Table 1. *Right:* Pareto curves $C(w_m)$ for the same data where $C(w_m)$ represents the fraction of parties with a vote fraction larger than w_m (analogous to wealth). The x-axis corresponds to rescaled values $w_m/\langle w_m \rangle$ where $\langle w_m \rangle = 1/N_p$ is the average vote fraction (i.e. assuming w_m units such that $\sum_m w_m = 1$).

For a given set of wealth values/vote fractions $w_m = E_m = V_m$, we construct the Lorenz curve as the set of points $(h(m), w(m))$ $(m = 0, 1, \ldots, N)$ where $h(m) =$

$\sum_{k=0}^{m-1} \rho_k$ are the cumulated normalized fractions of households/parties and $w(m) = \sum_{k=0}^{m-1} w_k \rho_k / w_s$ are the cumulated wealth/vote fractions. Here, $w_s = \sum_m w_m \rho_m$ is the average wealth/vote fraction such that $h(0) = w(0) = 0$ and $h(N) = w(N) = 1$.

For the case of real election data, we use $\rho_m = 1/N_p$ and vote fractions $w_m = V_m = E_m$ taken from the databases [1–3]. Here N_p is the number of political parties/candidates having participated at a certain election of a given year. For EU elections, since 1994, we have mostly $20 \leq N_p \leq 41$ (with a few cases of $N_p \sim 13 - 15$) and for the first round FR presidential election since 1965 we have $6 \leq N_q \leq 16$. (see Table 1).

For the case of a thermalized RJ model, using a certain simple model spectrum E_m with $0 = E_0 < E_1 < \ldots < E_{N-1} = B$ with some large value $N \geq 10^4$ (or even $N \to \infty$ [9,10]), we compute the Lorenz curve in the same way using for ρ_m the RJ expression (1) and for $w_s = E = \varepsilon B$ the global energy which is a given parameter. In this case, it is assumed that there are N thermalized agents with energy levels E_k for their political power in society and that each party is represented by a certain fraction of them.

We mention that a possible condensation (for very low values of $\varepsilon \ll 1$) where a significant fraction of probability is concentrated on a few modes (or only one mode at $m = 0$) corresponds to $w(h) \approx 0$ for a rather large interval of $h \in [0, h_c]$. This naturally explains the appearance of a strong wealth inequality when a huge part of population is poor and a tiny oligarchic population fraction captures a big part of total wealth as it is described in [9,10,13]. We show that a somewhat similar situation may take place for the party vote distribution in certain EU elections.

We note that the construction procedure of Lorenz curves is invariant with respect to global rescaling of $E_m \to \alpha E_m$ and $E \to \alpha E$. Therefore, we can choose model spectra with $B = 1$ such that $\varepsilon = E$. In [9,10], two specific spectral models were considered. The first one is based on the simple assumption that the density of energy states $\nu(k) = dk/dE_k$ is constant such that $0 \leq E_k = k/N < B = 1$ for $k = 0, 1, 2, ..., N-1$. This case is called the RJ standard (RJS) model [9, 10, 18]. The second case is the RJ extended (RJE) model with $E_k = (e^{ak/N} - 1)/(e^a - 1)$ where a is an additional real valued model parameter (the limit $a \to 0$ reproduces the RJS model). For $a > 0$, the density of states decreases at high energies with $\nu(E_k) = dk/dE_k = N(e^a - 1)/[a(1 + (e^a - 1)E_k]$. In both cases, the global energy scale is chosen such that $B = E_{N-1} \approx 1$.

For many typical cases studied in [9,10], e.g. Lorenz curves of household wealth in the World or countries, GPD of countries, stock market capitalization of companies etc., the RJE model describes very well real curves with typical optimal values of $a \sim 4$. In these cases, the simple RJS model (i.e. $a = 0$) gives only an approximate agreement woth data while the RJE curve typically matches the real data very well. However, in this work, for the cases of election Lorenz curves, we usually have small a values and the resulting Lorenz curves for the RJE model are very close to the RJS curves. We point that as in [9,10], when comparing real data with the RJS or RJE model, the value of ε is determined such that the Gini coefficient of the RJ model coincides with its value from the real data.

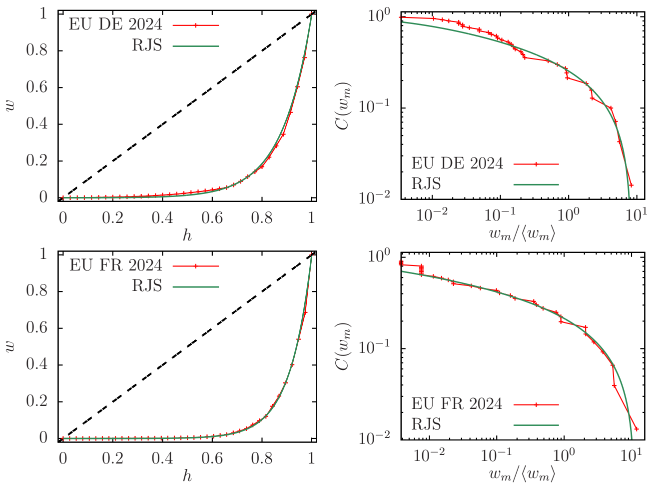

Fig. 2: (Color on-line) As Fig. 1 for the EU 2024 elections of DE (top) and FR (bottom). In addition, to the real data (red points) also the (green) theoretical RJS Lorenz curves (left panels) are shown (see Table 1 for specific values of G, ε and N_p). For the Pareto curves (right panels) the average $\langle w_m \rangle$ is either $1/N_p$ (real data) or ε (RJS curves). See also SupMat Figs. S1 and S2 for similar figures for the DE/FR EU elections of 1994 (Fig. S1) and 2014 (Fig. S2) (these Figs. also show curves for RJE model being very close to the RJS ones).

In addition to the Lorenz curve, we also study the cumulative distribution function (CDF) $C(w_m)$ that presents the fraction of households (parties) having a wealth/vote larger than $w_m = V_m$. For convenience, we call this function Pareto distribution (Pareto curve), even for more general cases where it does not obey an expected power law. The Pareto curve highlights in a better way the properties of high revenues (see e.g. [32]). For both cases of real data and RJ models, the Pareto curve is easily obtained by drawing $C(w_m) = 1 - h(w_m)$ as a function of the individual household wealth less than w_m. Here $h(w_m)$ corresponds to the fraction of (poorest) households having each an individual household wealth less than w_m. However, in contrast to the Lorenz curve, the Pareto curve still depends on a scale parameter for the units of w_m. In this work, we always show $C(w_m)$ as a function of the rescaled quantity $w_m/\langle w_m \rangle$ where $\langle w_m \rangle$ is the average "wealth" which is either directly known for real data or given by ε (for both RJ models with $B = 1$). For the case of elections, we simply have $\langle w_m \rangle = 1/N_p$ if w_m represents vote fractions normalized by $\sum_m w_m = 1$.

We mention, that the practical computation of Lorenz and Pareto curves for both RJ models (at given values of

ε and a), can be done very efficiently for quite large spectra $N \geq 10^4$ using the above construction procedure and numerically obtained values for μ and T as a function of ε. Furthermore, for the continuous limit $N \to \infty$ also explicit analytic formula for both $w(h)$ and $C(w_m)$ are available (see [10] for details). The RJ curves shown in this work were all computed for this continuous limit but curves for finite $N = 10^4$ are identical on graphical precision (with relative deviations $\sim 10^{-4}$).

Data. – In this work, we consider all 7 EU elections of DE and FR between 1994 and 2024, the latest 2024 EU elections of other 8 countries, IT, ES, PL, RO, NL, BE, SE, CZ (decreasing order of population) and also all 11 French 1st round presidential elections since 1965 using data of [1–3].

The main parameters of these elections, being the Gini coefficient G, obtained RJS value of ε from the given G value of each election, and the number N_p of political parties or French presidential first round candidates having participated are given in Table 1.

Results. – In Fig. 1, we show Lorenz and Pareto curves for Germany (top row) and France (bottom row) for 7 EU elections from years 1994 to 2024.

For Germany these distributions remain stable and there are only modest variations for the full period. The number of competing parties is between 23 (1999) and 41 (2019).

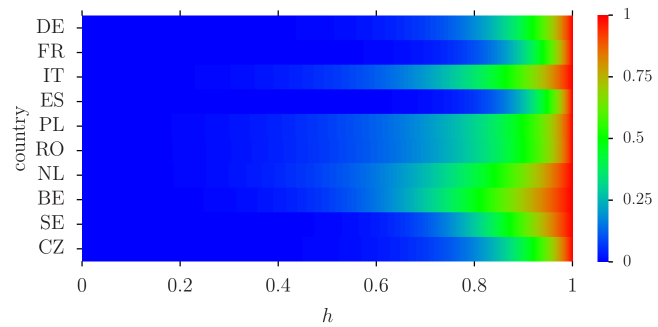

Fig. 3: (Color on-line) Density color plot of Lorenz curves for 10 countries (2024 EU elections) obtained from the RJS model for the 6 countries DE, FR, IT, ES, NL, CZ and from the optimal RJE model for the 4 countries PL, RO, BE, SE (cases with a visible difference between RJS and optimal RJE curve). The x-axis corresponds to the cumulated fraction of households/political parties (h) and the y-axis to the countries (with order of increasing population from bottom to top). The color value according to the colorbar shows the cumulated fraction of wealth/obtained votes (w). See also SupMat Figs. S3-S6 for figures in the style of Fig. 2 with Lorenz and Pareto curves for the 2024 EU elections of 8 EU countries (CZ to IT).)

For France the curves for 1994 and 1999 have visible deviations and smaller Gini coefficients than the other years which may be related to the reduced number of political parties $N_p = 20$ for these two years while for the other years $N_p \geq 27$ with maximal value $N_p = 39$ for 2004.

Table 1: Summary of parameters of certain EU and (first round) FR presidential elections (PR FR). The columns correspond to the type of election, year of election, Gini coefficient G, RJS rescaled energy ε, obtained by matching G between real data and the theoretical RJS Lorenz curve, and the number N_p of political parties or (first round) presidential candidates having participated at the election.

type	year	G	ε	N_p
EU DE	1994	0.802	0.099	26
EU DE	1999	0.820	0.090	23
EU DE	2004	0.772	0.115	24
EU DE	2009	0.800	0.100	32
EU DE	2014	0.766	0.118	25
EU DE	2019	0.810	0.095	41
EU DE	2024	0.763	0.119	35
EU FR	1994	0.635	0.194	20
EU FR	1999	0.597	0.219	20
EU FR	2004	0.816	0.092	39
EU FR	2009	0.765	0.118	27
EU FR	2014	0.752	0.125	31
EU FR	2019	0.783	0.109	34
EU FR	2024	0.824	0.088	38
EU IT	2024	0.625	0.200	15
EU ES	2024	0.848	0.076	34
EU PL	2024	0.654	0.181	20
EU RO	2024	0.658	0.179	13
EU NL	2024	0.574	0.236	20
EU BE	2024	0.551	0.255	22
EU SE	2024	0.696	0.156	20
EU CZ	2024	0.769	0.116	30
PR FR	1965	0.530	0.272	6
PR FR	1969	0.548	0.257	7
PR FR	1974	0.742	0.130	12
PR FR	1981	0.539	0.264	10
PR FR	1988	0.507	0.292	9
PR FR	1995	0.404	0.403	9
PR FR	2002	0.456	0.343	16
PR FR	2007	0.613	0.208	12
PR FR	2012	0.560	0.247	10
PR FR	2017	0.548	0.257	11
PR FR	2022	0.573	0.237	12

It is important to note that the Pareto curves in Fig. 1 clearly do not show an expected algebraic decay over a significant interval of w_m (see e.g. [32] and Refs. therein).

In global, these Lorenz and Pareto curves remain stable on a scale of the last 30 years for Germany and 20 years for France that indicates a certain stable mechanism behind. Below, we present arguments that this mechanism is related to RJ thermalization and condensation.

For example for the 2024 EU elections of DE and FR, Fig. 2 shows that the real data Lorenz and Pareto curves agree very well with the corresponding theoretical curves obtained from the RJS model using the above construction procedure with the RJ expression (1) for ρ_m and a uniform density of states for the spectrum E_m. This is also confirmed, by the similar SupMat Figs. S1 and S2 for 1994 and 2014 EU elections of DE and FR; also for these years RJS and RJE curves are very close.

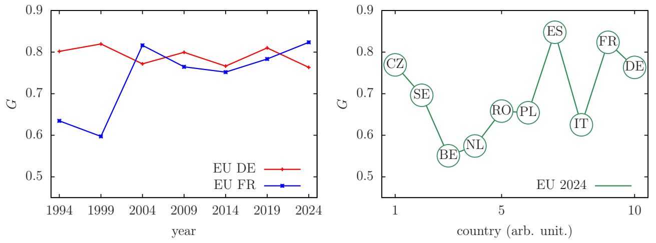

Fig. 4: (Color on-line) *Left:* Dependence of the Gini coefficient G for the EU elections of DE (red) and FR (blue) on the election year (using the same data as in Fig. 1). *Right:* Gini coefficient G for the EU elections 2024 for 10 European countries (green) ordered with increasing size of population (from left to right; using the same data as in Fig. 3).

In Fig. 3, we show a collection of all Lorenz curves for the 2024 EU elections of the 10 most populated EU countries for either the RJS model (6 cases) or the RJE model with optimal value of a (4 cases) as a density color plot. For all these cases, the shown RJ curves agree very well with the real data curves as can be seen in SupMat Figs. S3-S6 (for the 4 cases with RJE curves in Fig. 3 there is some visible difference between the RJE/real data curve and the corresponding RJS curve and here we have larger optimal values of a with $|a| > 2$). Here the number of political parties N_p is rather small for RO (13) and IT (15), intermediate for PL, NL, BE and SE (20-22) and somewhat larger for CZ (30), ES (34), DE (35) and FR (38).

Fig. 4, shows the dependence of the Gini coefficient G for the DE/FR EU elections on the election year between 1994 and 2024 (left panel) and for the 2024 EU elections of the 10 most populated EU countries on the country index (defined by order of increasing population).

For FR 1994/1999 there are some deviations with smaller values of $G \approx 0.6$, also visible in Fig. 1 on a qualitative level, and corresponding RJS values of $\varepsilon \approx 0.2$. For the other years of FR and all years of DE, we have typically $G \approx 0.8$ and $\varepsilon \approx 0.1$, indicating lower temperatures and the emergence of a (stronger) RJ condensation. In particular, from the RJS Lorenz curves of Fig. 2 we see for DE (FR) that 50% of bottom parties gain approximately only 1.4% (0.3%) of total votes while top 10% of parties gain approximately 57% (68%) of total votes. These values are comparable with those of wealth inequality for the whole world in 2021 with $G = 0.842$ [7, 9]. However, the World 2021 Lorenz curve analyzed in [10] requires a large RJE parameter $a = 4.74$ and there the RJS curve does not match very well the real data, In contrast for the FR/DE 2024 EU election Lorenz curves are well described by the RJS model..

For the other 8 EU elections of 2024 the Gini coefficients vary between $G \approx 0.55$ (BE with $\varepsilon \approx 0.26$) and $G \approx 0.85$ (ES with $\varepsilon \approx 0.076$). Globally, G decreases with increasing ε (increasing temperature). The analytic theory of the RJS model for $N \to \infty$ [9, 10] gives for $\varepsilon \leq 0.2$ the quite good approximation $G \approx 1 - 2\varepsilon$ (the complete data of SupMat Table S1 is quite well fitted by $G \approx 1 - 2\varepsilon + 3.4\,\varepsilon^3$ for the larger interval $\varepsilon \in [0, 0.4]$).

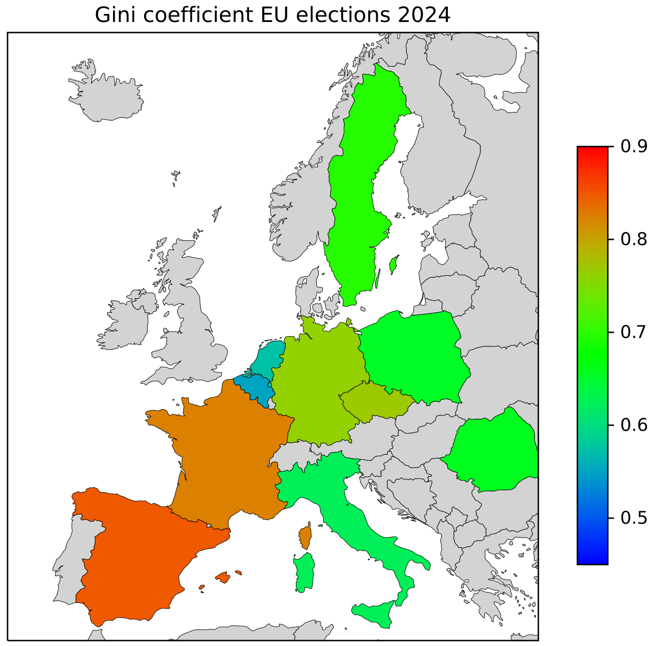

Fig. 5: (Color on-line) Europe map color plot of the Gini coefficient of the EU elections of 2024 of 10 countries using the data of the right panel of Fig. 4.

The Gini coefficients of the 10 most populated EU countries are also illustrated in the Europe map color plot of Fig. 5. We note that the values of G for the 10 countries, visible in the right panel of Fig. 4 and in Fig. 5, also agree on a qualitative level with the RJ Lorenz curves in the color plot of Fig. 3, i.e. the length of the green/red zone in Fig. 3 increases with decreasing values of G.

Finally, it is important to note that the TTV approach works not only for elections of parties but also for elections of individual candidates if their number is not too small. As examples, we consider the case of the first round French presidential elections using data from [3], where typically a significant number of candidates participate, even though this number, typically 9-12 for most years and with extreme values between 6 (1965) and 16 (2002), is quite smaller than the number of parties of typical EU elections.

However, Fig. 6 still shows a very good agreement between the real data and the theoretical RJS Lorenz and Pareto curves for the 2022 election. SupMat Figs. S7-S11 provide rather similar results for the other 10 elections from 1965 to 2017. The dependence of the Gini coefficients for the 11 first round presidential elections between 1965

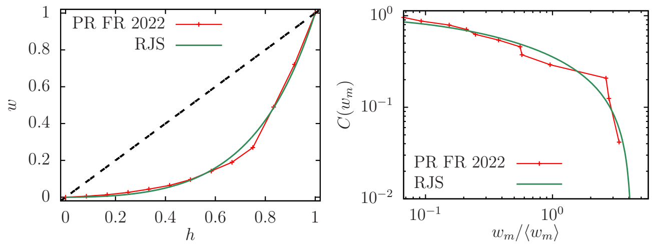

Fig. 6: (Color on-line) Same style as Fig. 2 but for the first round FR presidential election of 2022. See also SupMat Figs. S7-S11 for similar figures for the first round FR presidential elections between 1965 and 2017 (10 elections) and SupMat Fig. S12 for the dependence of the Gini coefficient of all FR first round presidential since 1965 on the election year (11 elections). In all cases, the parameter values for G, ε and N_p are available in Table 1.

and 2022 on the election year is shown in SupMat Fig. S12. Here, typically G is mostly in the interval $G \in [0.45, 0.6]$ with exceptions for 1995 ($G \approx 0.4$) and 1974 ($G \approx 0.74$). These values are globally quite smaller as for most EU elections, which can be explained by the reduced value of N_p such that a strong inequality is less likely. The dependence of G on the RJS rescaled energy ε (obtained by matching G between the real data and the RJS Lorenz curves) is the same as already given above, but since most typical G (or ε) values are smaller (larger) in comparison to the EU elections, the more general 3rd order fit needs to be used for most data points.

Discussion. – In this work, we introduce the TTV approach which describes very well the statistical distribution of votes for parties participating in EU elections during the last 30 years and for candidates of the first round French presidential elections since 1965. The theory is based on RJ thermalization with possible condensation which has been observed in other physical systems such as in multimode optical fibers [14–18]. The RJ condensation appears for a low total system energy when a macroscopic fraction of probability is concentrated in a vicinity of the ground state energy. A similar phenomenon is also known as the constraint driven condensation in statistical mechanics of various classical systems [19–21]. In the context of wealth inequality in the world, this RJ condensation [9, 10] explains a huge poverty phase and a tiny oligarchic phase observed for many world countries [6, 7]. More recently, it was shown that the RJ approach also describes well energy and carbon emission distributions between countries [13]. In this work, we extended this approach to the statistical distribution of vote fractions in elections confirming that it describes well EU and French first round presidential elections. In the context of elections a possible RJ condensation corresponds to the appearance of a large fraction of parties that cumulate a very small percent of total votes while few top parties accumulate a big fraction of total votes.

The observation that RJ thermalization, applies to many statistical steady-state distributions in physical and social systems confirms its universal nature for these systems.

The TTV approach can be also applied to other types of elections, e.g. for elections of various committees in companies, or local elections. Of course, the TTV description only provides a general physical constraint for typical vote distributions but does not tell who will win an election.

Acknowledgments: The authors acknowledge support from the grant ANR France project NANOX $N°$ ANR-17-EURE-0009 in the framework of the Programme Investissements d'Avenir (project MTDINA). This work was granted access to the HPC resources of CALMIP (Toulouse) under the allocation 2026-P0110.

Data Availability Statement: The research data associated with this article are included within the article and the used raw data is available in [1–3].

REFERENCES

[1] Wikipedia contributors. *Elections to the European Parliament*, `https://en.wikipedia.org/wiki/Elections_to_the_European_Parliament` (Accessed July 3, 2026).

[2] EU Parliament, `https://elections.europa.eu/en/how-elections-work/` (Accessed June 25, 2026).

[3] Wikipedia contributors. *French presidential elections under the Fifth Republic* `https://en.wikipedia.org/wiki/French_presidential_elections_under_the_Fifth_Republic` (Accessed July 3, 2026).

[4] Lorenz M.O. Methods of measuring the concentration of wealth. Quarterly Publications of the American Statistical Association, **1905**, *9*, 209 (New Series, No. 70); `https://doi.org/10.1080/15225437.1905.10503443` (Accessed June 25, 2026).

[5] Gini C. Sulla misura della concentrazione e della variabilit'a dei caratteri. Atti del Reale Istituto Veneto di Scienze, Lettere ed Arti 1914; 73: 1203; English translation in Metron - Int. J. Statistics **63** (2005) 3; `https://www.dss.uniroma1.it/RePec/mtn/articoli/2005-1-1.pdf` (Accessed June 25, 2026).

[6] Piketty T. Capital in the Twenty-First Century. Belknap Press of Harvard University Press, Cambridge, MA (2014).

[7] Chancel L., Piketty T., Saez E., and Zucman G. *et al.*. World Inequality Report)2022). World Inequality Lab `https://wir2022.wid.world` (Accessed on June 25, 2026).

[8] Roach B., Rajkanikar P.J., Goodwin N., and Harris J. Social and Economic Inequality. An ECI Teaching Module on Social and Environmental Issues, Economics in Context Initiative, Global Development Policy Center, Boston University (2003), `https://www.bu.edu/eci/files/2023/05/Inequality-Module-2023.pdf` (Accessed June 25, 2026).

[9] Frahm K.M., and Shepelyansky D.L. *Wealth thermalization hypothesis and social networks*, arXiv:2506.17720 [cond-mat.stat-mech] (2025); J. Stat. Phys. **193** (2026) 64.

[10] Frahm K.M., Ermann L. and Shepelyansky D.L. *Thermodynamic description of wealth inequality in the world*, arXiv:2606.17965[cond-mat.stat-mech] (2026).

[11] Landau L.D., and Lifshitz E.M.. *Statistical physics*, Elsvier, Amsterdam (1980).

[12] Zakharov V.E., L'vov V.S., and Falkovich G. *Kolmogorov spectra of turbulence I*, Springer, Berlin (1992).

[13] Frahm K,M, and Shepelyansky D.L. *Thermodynamic description of worldwide distribution of energy and carbon emission*, arXiv:2607.07315 (2026).

[14] Krupa K., Tonello A., Barthelemy A., Shalaby B.M., Bendahmane A., Millot G., and Wabnitz S., *Observation of geometric parametric instability induced by the periodic spatial self-imaging of multimode waves*, Phys. Rev. Lett. **116** (2016) 183901.

[15] Connaughton C., Josserand C., Picozzi A., Pomeau Y., and Rica S., *Condensation of classical nonlinear waves*, Phys. Rev. Lett. **95** (2005) 263901.

[16] A. Picozzi A., Garnier J., Hansson T., Suret P., Randoux S., Millot G., and Christodoulides D.N., *Optical wave turbulence: Towards a unified nonequilibrium thermodynamic formulation of statistical nonlinear optics*, Phys. Rep. **542** (2014) 1.

[17] Baudin K., Fusaro A., Krupa K., Garnier J., Rica S., Millot G., and Picozzi A., *Classical Rayleigh-Jeans condensation of light waves: observation and thermodynamic characterization*, Phys. Rev. Lett. **125** (2020) 244101.

[18] Ermann L., Chepelianskii A.D., and Shepelyansky D.L., *Dynamical thermalization, Rayleigh-Jeans condensate, vortexes and wave collapse in quantum chaos fibers and fluid of light*, J. Phys. A: Math. Theor. **59** (2026) 055702.

[19] Evans M.R., Majumdar S.N., Pagonabarraga I., and Trizac E., *Condensation transition in polydisperse hard rods*, J. Chem. Phys. **132** (2010) 014102.

[20] Szavits-Nossan J., Evans M.R., and Majumdar S.N., *Constraint driven condensation in large fluctuations of linear statistics*, Phys. Rev. Lett. **112** (2014) 020602.

[21] Filiasi M., Livan G., Marsili M., Peressi M., Vesselli E., and Zarinelli E., *On the concentration of large deviations for fat tailed distributions, with application to financial data*, J. Stat. Mech. (2014) P09030.

[22] Frahm K.M. and Shepelyansky D.L. *Dynamical thermalization and turbulence in social stratification models*, CHAOS **36** (2026) 073117.

[23] Rabinowitz G. and Macdonald S.E. *A Directional Theory of Issue Voting*, American Polit. Sci. Rev. **83(1)** (1989) 93.

[24] Myerson R.B. and Weber R.J. *A theory of voting equilibria*, American Polit. Sci. Rev. **87(1)** (1993) 102.

[25] Coughlin P.J. *Probabilistic voting theory*, Cambridge Univ. Press, Cambridge UK (2003).

[26] Slomczynski W. and Zyczkowski K. *Mathematical aspects of degressive proportionality*, Math. Social Sci. **63** (2012) 94.

[27] Sznajd-Weron K. and Sznajd J. *Opinion evolution in closed community*, Int. J. Modern Physics C **11** (2000) 1157.

[28] Sood V. and Redner S. *Voter Model on Heterogeneous Graphs*, Phys. Rev. Lett. **94** (2005) 178701.

[29] Galam S. *Sociophysics: a review of Galam models*, Int. J. Modern Physics C **19** (2008) 409.

[30] Bukina K. and Shepelyansky D.L. *Opinion formation at Ising social networks*, Entropy **17** (2026) 41.

[31] Dragulescu A. and Yakovenko V. *Statistical mechanics of money*, Eur. Phys. J. B. **17** (2000) 723.

[32] Yakovenko V.M. and Rosser J.B. *Colloquium: Statistical mechanics of money, wealth, and income*, Rev. Mod. Phys. **81** (2009) 1703.

[33] Boghosian B.M., Devitt-Lee A., Johnson M., Li J., Marcq J.A., and Wang H., *Oligarchy as a phase transition: the effect of wealth-attained advantage in a Fokker–Planck description of asset exchange*, Physica A **476** (2017) 15.

[34] Boghosian B.M., *The inescapable casino*, Sci. American, November (2019) 71.

Supplementary Material for

Thermodynamic theory of voting and EU elections

by K. M. Frahm and D. L. Shepelyansky
Laboratoire de Physique Théorique, Université de Toulouse, CNRS, UPS, 31062 Toulouse, France

Here, we present additional figures and additional information. We remind that Table 1, gives for all elections discussed in this work a summary of the 3 parameters G (Gini coefficient), ε (rescaled energy for the RJS Lorenz curve obtained by matching G with the real data Lorenz curve) and the number N_p of political parties (EU elections) or candidates for the (first round) FR presidential election. Since these values are available in Table 1, they are not mentioned in the figure captions of the figures of the main part or other figures given below.

In certain cases, we provide for illustration or due to visible deviations between the RJE and RJS cases also RJE Lorenz and Pareto curves with values of the optimal parameter a (which minimizes the geometrical Lorenz curve distance with respect to the real data) and the associated value of $\varepsilon_{\rm RJE}$ (which may deviate from ε of the RJS model given in Table 1).

The following figures concern (mostly) additional figures in the style of Fig. 2 (except Fig. S12; see below).

More specifically, Figs. S1 and S2 concern the EU elections of DE/FR of 1994 (Fig. S1) and of 2014 (Fig. S2) both also with RJE curves (blue) for illustration.

Figs. S3-S6 concern the EU elections of 2024 of 8 countries other than DE or FR (from the list of 10 countries used in the main part and in Figs. 3-5). Here, in four cases with visible deviations between the RJE and RJS models, also curves and parameter values for the RJE case are given (see also caption of Fig. 3 for the list of countries where RJE curves are shown).

Figs. S7-S11 concern the 10 first round FR presidential elections of the years 1965 to 2017 (the case of 2022 is shown in Fig. 6 of the main part).

Finally, Fig. S12 shows the dependence of the Gini coefficient on the election year for the 11 first round FR presidential elections of the years 1965 to 2022.

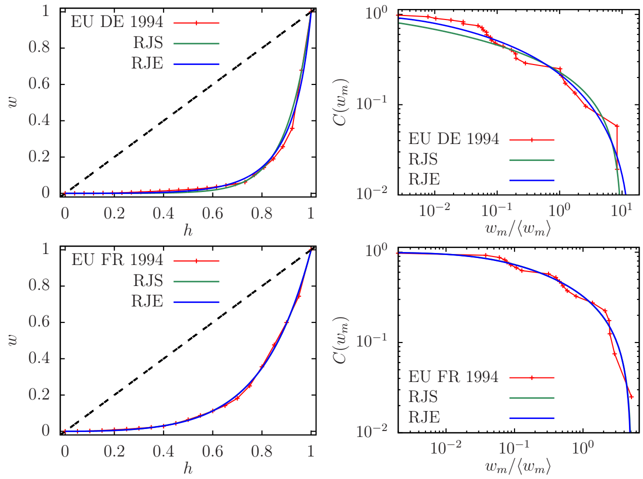

Fig. S1: As Fig. 2 for the EU election of DE/FR of 1994. For illustration also the theoretical RJE curves are shown (blue). The optimal RJE parameters are $a = 1.25$, $\varepsilon_{\rm RJE} = 0.069$ (EU DE 1994) and $a = -0.0701$, $\varepsilon_{\rm RJE} = 0.196$ (EU FR 1994).

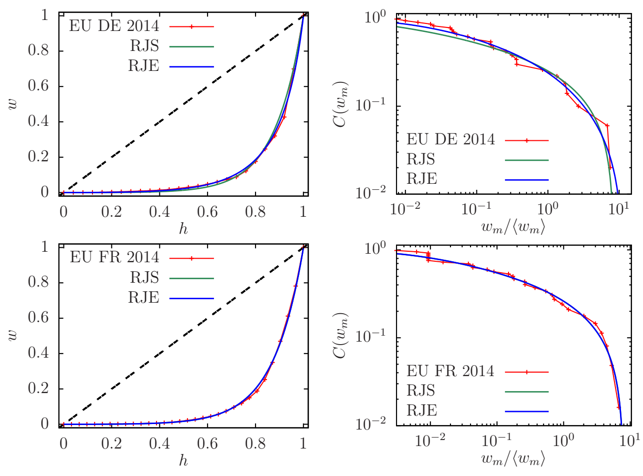

Fig. S2: As Fig. 2 for the EU election of DE/FR of 2014. For illustration also the theoretical RJE curves are shown (blue). The optimal RJE parameters are $a = 1.07$, $\varepsilon_{\rm RJE} = 0.0875$ (EU DE 2014) and $a = 0.00573$, $\varepsilon_{\rm RJE} = 0.125$ (EU FR 2014).

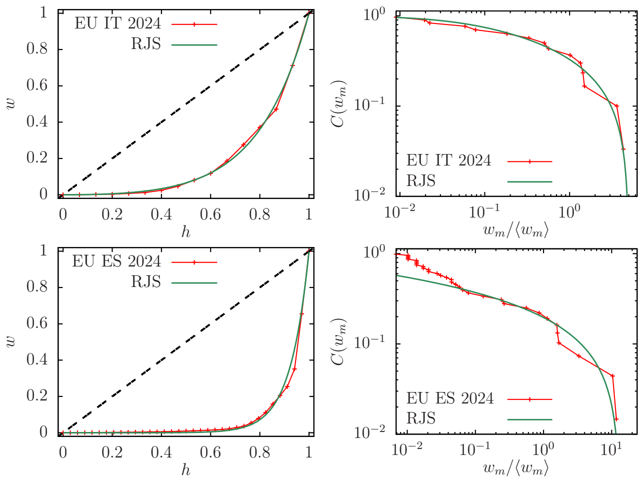

Fig. S3: As Fig. 2 for the EU election of IT/ES of 2024.

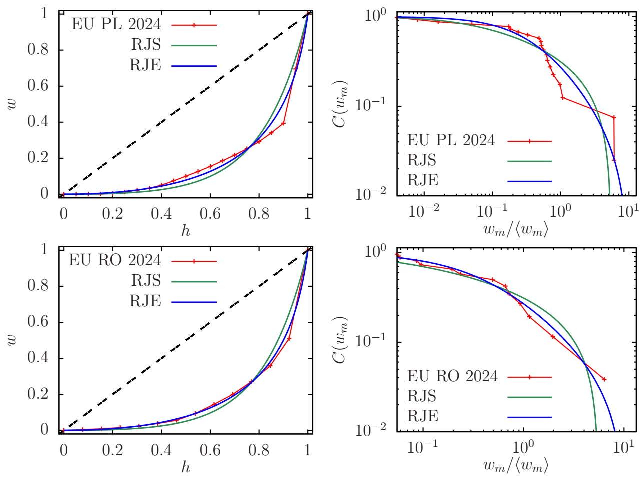

Fig. S5: As Fig. 2 for the EU election of PL/RO of 2024. For both cases also the theoretical RJE curves are shown (blue) and the optimal RJE parameters are $a = 3.16$, $\varepsilon_{\rm RJE} = 0.102$ (EU PL 2024) and $a = 3.22$, $\varepsilon_{\rm RJE} = 0.0982$ (EU RO 2024).

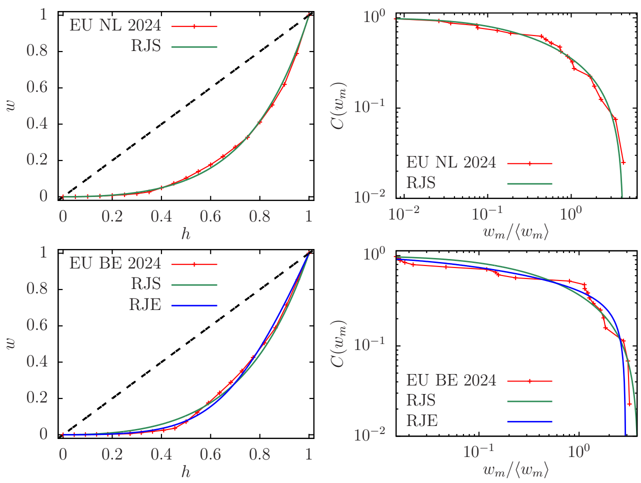

Fig. S4: As Fig. 2 for the EU election of NL/BE of 2024. For BE also the theoretical RJE curves are shown (blue) and the optimal RJE parameters are $a = -2.35$, $\varepsilon_{\rm RJE} = 0.342$.

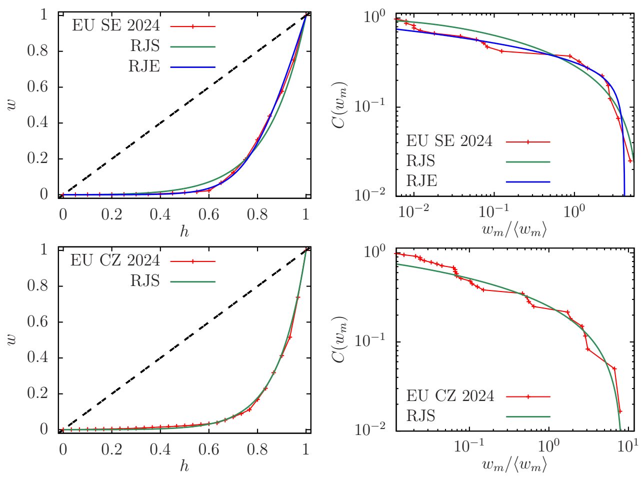

Fig. S6: As Fig. 2 for the EU election of SE/CZ of 2024. For SE also the theoretical RJE curves are shown (blue) and the optimal RJE parameters are $a = -2.69$, $\varepsilon_{\rm RJE} = 0.236$.

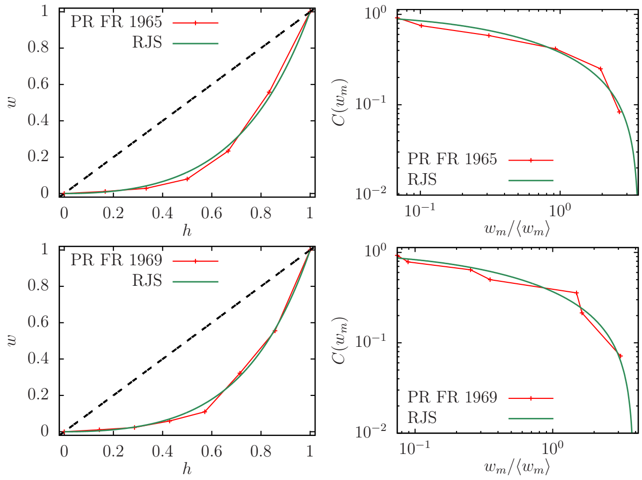

Fig. S7: As Fig. 6 but for the first round FR presidential elections of 1965 and 1969.

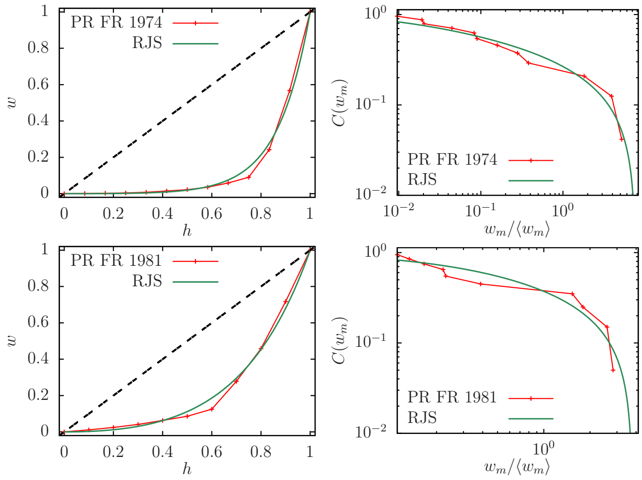

Fig. S8: As Fig. 6 but for the first round FR presidential elections of 1974 and 1981.

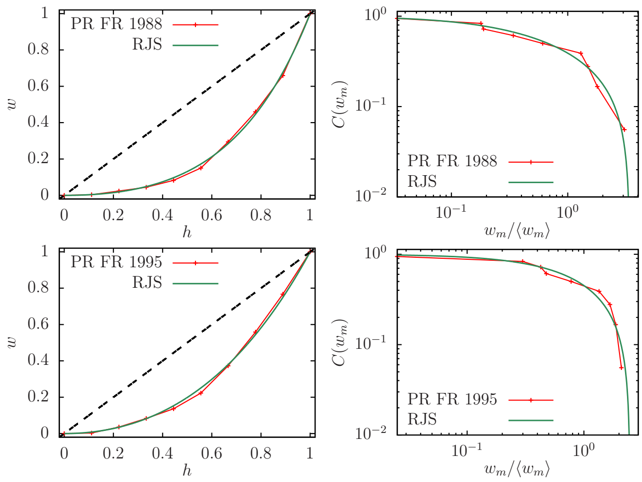

Fig. S9: As Fig. 6 but for the first round FR presidential elections of 1988 and 1995.

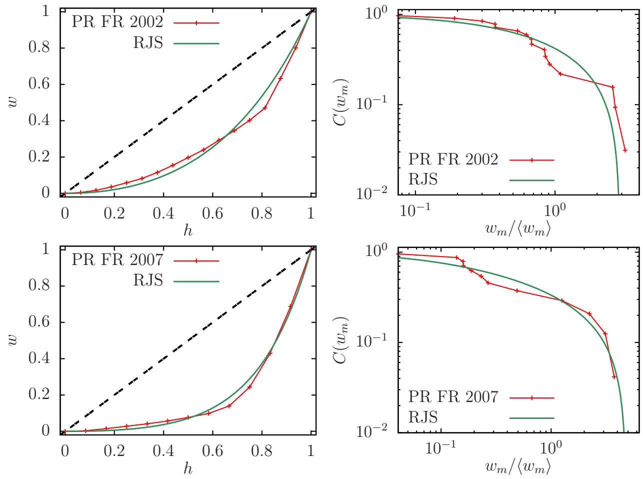

Fig. S10: As Fig. 6 but for the first round FR presidential elections of 2002 and 2007.

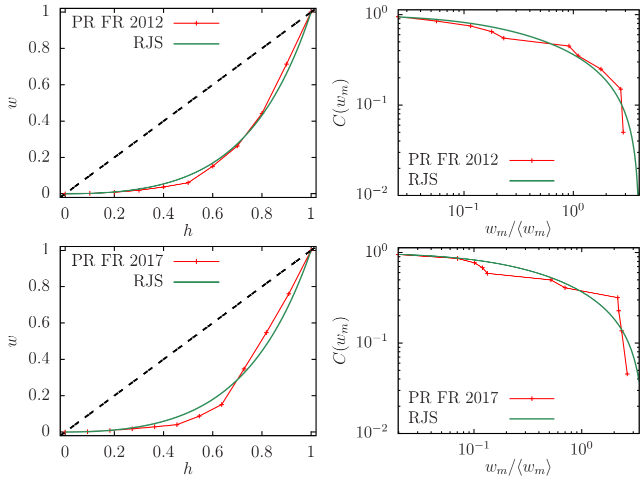

Fig. S11: As Fig. 6 but for the first round FR presidential elections of 2012 and 2017.

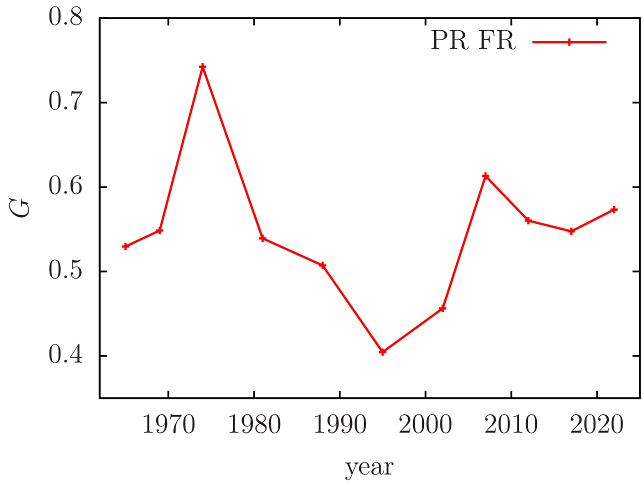

Fig. S12: Dependence of the Gini coefficient of all FR first round presidential since 1965 on the election year (11 elections).